nature genetics



# Impaired microRNA processing enhances cellular transformation and tumorigenesis

Madhu S Kumar[1], Jun Lu[2,3], Kim L Mercer[1], Todd R Golub[2–4] & Tyler Jacks[1,5]

**MicroRNAs (miRNAs) are a new class of small noncoding RNAs that post-transcriptionally regulate the expression of target mRNA transcripts. Many of these target mRNA transcripts are involved in proliferation, differentiation and apoptosis[1,2], processes commonly altered during tumorigenesis. Recent work has shown a global decrease of mature miRNA expression in human cancers[3]. However, it is unclear whether this global repression of miRNAs reflects the undifferentiated state of tumors or causally contributes to the transformed phenotype. Here we show that global repression of miRNA maturation promotes cellular transformation and tumorigenesis. Cancer cells expressing short hairpin RNAs (shRNAs) targeting three different components of the miRNA processing machinery showed a substantial decrease in steady-state miRNA levels and a more pronounced transformed phenotype. In animals, miRNA processing–impaired cells formed tumors with accelerated kinetics. These tumors were more invasive than control tumors, suggesting that global miRNA loss enhances tumorigenesis. Furthermore, conditional deletion of *Dicer1* enhanced tumor development in a K-Ras–induced mouse model of lung cancer. Overall, these studies indicate that abrogation of global miRNA processing promotes tumorigenesis.**

In order to examine the role of miRNA processing in tumorigenesis, we designed shRNAs targeting the three established regulators of miRNA processing: Drosha, DGCR8 and Dicer1. In mouse lung adenocarcinoma (LKR13) cells[4,5], these hairpins achieved robust knockdown of target mRNA levels (**Fig. 1a**) and reduced steady-state miRNA levels (**Fig. 1b**). Of note, these shRNAs did not completely eliminate mature miRNAs. For Dicer1 in particular, we would expect incomplete knockdown, as Dicer1 is required for the generation of its target small interfering RNA. We then tested the effect of impaired miRNA processing on the transformation properties of these cells. miRNA processing–impaired cells (hereafter referred to as 'miRKD') LKR13 cells formed substantially larger colonies than controls did when we plated them at low density (**Fig. 1c**) and had improved colony formation in soft agar (**Supplementary Fig. 1** online). Additionally, miRKD cells formed more foci than control cells (**Supplementary Fig. 1**). These enhanced transformation properties seem to be a consequence of increased proliferation, as miRKD cells grew faster than controls and showed a higher percentage of cells entering S phase and a reduced number of $G_0/G_1$ cells (**Supplementary Fig. 1**). Thus, defective miRNA maturation (or some other unknown function of these genes) alters the transformed state of mouse tumor cells, accompanied by enhanced proliferative capacity.

To determine if impaired miRNA processing affected mouse and human cancer cells similarly, we designed additional short hairpin RNAs against the human miRNA processing machinery. These hairpins also achieved knockdown of steady-state miRNA levels in three independent human cancer cell lines as assessed by RNA blotting (**Fig. 1d**) and miRNA profiling (**Supplementary Table 1** online). Similar to the results from LKR13 cells, impaired miRNA processing enhanced both colony formation and growth in soft agar of human cancer cells (**Fig. 1e** and **Supplementary Fig. 1**). Notably, this effect was independent of the tissue of origin; miRKD cells derived from osteosarcomas (U2OS), colorectal carcinomas (HCA7) and breast carcinomas (MCF7) all showed enhanced transformation (**Fig. 1e** and **Supplementary Fig. 1**). Overall, these results suggest that global repression of miRNAs enhances transformation of cancer cells.

To determine if global repression of miRNAs enhances the tumorigenic potential of cancer cells, we injected miRKD LKR13 cells subcutaneously into immunocompromised mice. miRKD cells formed tumors with accelerated kinetics, with tumor volumes that were at least an order of magnitude greater than in controls (**Fig. 2a**). Steady-state miRNA levels in miRKD tumors were lower than those in controls (**Supplementary Fig. 2** online). Earlier work suggested that the global loss of miRNAs in human cancers corresponds to altered differentiation in tumors relative to normal tissue[3]. Thus, it was possible that miRKD tumors might be histologically distinct from controls. We were surprised to find that miRKD tumors were similar to controls by histological analysis; all appeared moderately differentiated, with the clear presence of glandular structures (**Supplementary Fig. 2**). Notably, however, miRKD tumors commonly

[1]MIT Center for Cancer Research, Cambridge, Massachusetts 02139, USA. [2]Broad Institute of MIT and Harvard, Cambridge, Massachusetts 02141, USA. [3]Department of Pediatric Oncology, Dana-Farber Cancer Institute and Harvard Medical School, Boston, Massachusetts 02115, USA. [4]Howard Hughes Medical Institute, Harvard Medical School, Boston, Massachusetts 02115, USA. [5]Howard Hughes Medical Institute, Department of Biology, Massachusetts Institute of Technology, Cambridge, Massachusetts 02139, USA. Correspondence should be addressed to T.J. (tjacks@mit.edu).

Received 4 December 2006; accepted 12 February 2007; published online 1 April 2007; doi:10.1038/ng2003

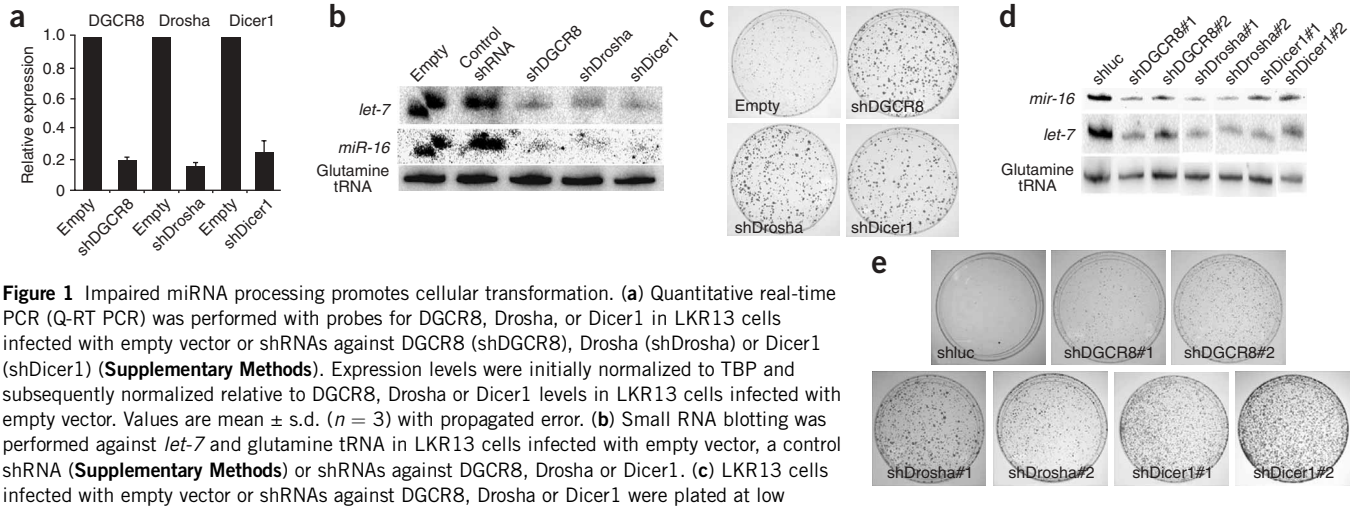


**Figure 1** Impaired miRNA processing promotes cellular transformation. (**a**) Quantitative real-time PCR (Q-RT PCR) was performed with probes for DGCR8, Drosha, or Dicer1 in LKR13 cells infected with empty vector or shRNAs against DGCR8 (shDGCR8), Drosha (shDrosha) or Dicer1 (shDicer1) (**Supplementary Methods**). Expression levels were initially normalized to TBP and subsequently normalized relative to DGCR8, Drosha or Dicer1 levels in LKR13 cells infected with empty vector. Values are mean ± s.d. ($n = 3$) with propagated error. (**b**) Small RNA blotting was performed against *let-7* and glutamine tRNA in LKR13 cells infected with empty vector, a control shRNA (**Supplementary Methods**) or shRNAs against DGCR8, Drosha or Dicer1. (**c**) LKR13 cells infected with empty vector or shRNAs against DGCR8, Drosha or Dicer1 were plated at low density (2500 cells per 10 cm plate), grown for 5 d and fixed and stained with crystal violet. (**d**) Small RNA blotting was performed as above in U2OS cells infected with shRNAs against *Renilla* luciferase, DGCR8, Drosha or Dicer1. We generated two independent shRNAs (numbered 1 and 2) specific for DGCR8, two specific for Drosha and two specific for Dicer1 (**Supplementary Methods**). (**e**) U2OS cells infected with shRNAs against *Renilla* luciferase, DGCR8, Drosha or Dicer1 were plated at low density as described above.



invaded the surrounding normal tissue of the host, including skeletal muscle, adipose tissue and nerve sheaths (**Fig. 2b**). Careful histological analysis of control tumors did not show any such invasion (data not shown). Consistent with the invasive phenotype in miRKD tumors, miRKD cells demonstrated enhanced migration through a collagen matrix *in vitro*, suggesting that repression of miRNAs in cancer cells results in increased motility (**Fig. 2c**).

Recent work with loss-of-function alleles of *Dicer1* in mammals has described defects in processes potentially unrelated to miRNAs, such as silencing of heterochromatic regions and chromosome segregation[6–8]. We did not observe any changes in transcript levels from major satellite repeats (**Supplementary Fig. 3** online); in addition, we noted similar levels of phosphorylated ribosomal S6 and eIF2α in miRKD and control cells, suggesting that global translation is not altered (**Supplementary Fig. 3**). However, it remained possible that miRKD cells had undergone irreversible changes (independent of miRNAs) that enhance transformation. To investigate this possibility, we generated a shRNA against Dicer1 flanked by loxP sites (pSico$^R$-shDicer1), allowing subsequent removal of the hairpin via Cre-mediated recombination[9]. Upon delivery of adenoviral Cre to pSico$^R$-shDicer1 cells, we observed a concomitant restoration of miRNA processing (**Supplementary Fig. 4** online). miRNA processing continued to be impaired in pSico$^R$-shDicer1 cells infected with a control adenovirus. Notably, adenoviral Cre-mediated removal of the Dicer1 hairpin resulted in reduced soft agar growth relative to control adenovirus-treated cells. We did not observe this reversal in pSico$^R$-shluc cells (**Supplementary Fig. 4** online). Thus, the enhanced transformation associated with impaired miRNA processing was reversible.

To determine if this enhanced transformation was specific to depletion of the miRNA processing machinery, we attempted to overcome the effect through expression of human cDNAs in miRKD LKR13 cells. As mouse shRNAs do not show full sequence complementarity with their human cDNA counterparts, we expected the human cDNAs to retain expression. In this context, miRNA processing would be maintained while the shRNA was expressed and functional. We observed a near-complete restoration of miRNA expression in cells containing the human cDNA in tandem with its target shRNA (**Supplementary Fig. 4**). Of note, shRNA-expressing cells lacking their corresponding cDNA or expressing a cDNA against a different miRNA processing component failed to restore mature miRNA levels, validating the specificity of the effect. The cells whose miRNA processing was rescued showed reductions in both low-density colony formation and growth in soft agar compared with miRKD cells (**Supplementary Fig. 4**), demonstrating that protection against impaired miRNA processing was sufficient to prevent the phenotype triggered by the shRNAs. Therefore, the enhanced transformation corresponding to defective miRNA maturation was specific to the miRNA processing machinery and was not a nonspecific effect of shRNA expression.

In order to test if impaired miRNA processing was sufficient to transform noncancerous cells, we expressed shRNAs against the

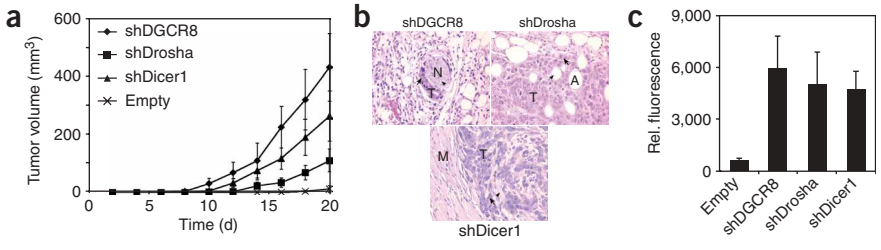


**Figure 2** Impaired miRNA processing promotes tumorigenesis *in vivo*. (**a**) LKR13 cells infected with empty vector or shRNAs against DGCR8, Drosha or Dicer1 were injected subcutaneously into immunocompromised mice ($10^5$ cells/injection), and tumor growth was measured over time. Values are mean ± s.e.m. ($n = 6$). (**b**) Hematoxylin/eosin staining of tumors, showing examples of tumor cells surrounding nerve sheaths and infiltrating into host adipose tissue and skeletal muscle of the host. Original magnification, 40×. N, nerve sheath. A, adipose tissue. M, skeletal muscle. T, tumor cells. Arrows indicate infiltrating tumor cells. Arrowheads indicate host tissue infiltrated by tumor cells. (**c**) *In vitro* migration assays using LKR13 cells infected with empty vector or shRNAs against DGCR8, Drosha or Dicer1 (see Methods). Results are representative of three replicates. Values are mean ± s.d. ($n = 3$).

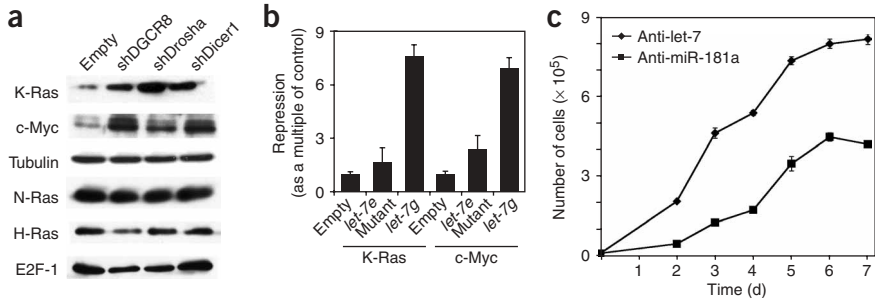


**Figure 3** Impaired miRNA processing increases expression of specific oncogenes. (**a**) Immunoblotting for K-Ras, c-Myc, α-tubulin, N-Ras, H-Ras and E2F-1 in LKR13 cells infected with empty vector or shRNAs against DGCR8, Drosha or Dicer1. (**b**) Luciferase assays were performed in 293T cells transfected with pRL-TK containing bulged siCXCR4 binding sites[28] or mouse K-Ras and c-Myc 3′ UTRs. pGL3 was used as a transfection control. Expression w as normalized to pGL3 levels and subsequently normalized relative to pRL-CXCR4 expression. Values are mean ± s.d. ($n = 6$) with propagated error. (**c**) LKR13 cells were transfected with 2′-*O*-methyl oligonucleotides complementary to either *miR-181a* or *let-7g* and were then plated at 5,000 cells per well. Cells were counted over time in triplicate. Values are mean ± s.e.m. ($n = 3$).



miRNA processing machinery in $Kras^{G12D}$-expressing mouse embryonic fibroblasts (MEFs), which have been shown to be incompletely transformed[10]. Compared with control $Kras^{G12D}$ MEFs, miRKD $Kras^{G12D}$ MEFs had an elevated growth rate (**Supplementary Fig. 5** online). However, impaired miRNA processing was not sufficient to fully transform $Kras^{G12D}$ MEFs, as evidenced by the inability of the cells to form colonies in soft agar (data not shown). To further address the role of miRNA processing on proliferation, we infected wild-type MEFs with shRNAs against the miRNA processing machinery and examined long-term population growth. Notably, wild-type cells had a markedly lower long-term proliferative capacity compared with controls (**Supplementary Fig. 5**), consistent with observations from *Dicer1*-null MEFs and embryonic stem cells[6–8]. Therefore, although defective miRNA biogenesis improves the transformation of cancer cells, it is not sufficient to promote *de novo* transformation.

To begin to investigate the basis for the enhanced transformation associated with repression of miRNAs, we measured the expression of several oncogenes in miRKD LKR13 cells. We detected substantially higher protein levels of the oncogenes c-Myc and K-Ras without changes in other known oncogenes such as N-Ras, H-Ras and E2F-1 (**Fig. 3a**). K-Ras mRNA levels were slightly elevated in miRKD cells, whereas c-Myc mRNA levels were unchanged compared with controls (**Supplementary Fig. 5**). As Ras family members have been shown to stabilize the c-Myc protein post-translationally through activation of the MEK/ERK and Akt signaling pathways[11], we investigated whether these pathways were altered in miRKD cells. Notably, there were no consistent changes in MEK1/2, ERK1/2 or Akt phosphorylation in response to impaired miRNA processing (**Supplementary Fig. 5**). These data suggest that miRNAs directly regulate c-Myc expression post-transcriptionally.

To examine potential miRNA-mediated regulation, we used the miRNA target prediction program miRanda[12] and observed that the 3′ UTRs of mouse K-Ras and c-Myc were both targets of the *let-7* family of miRNAs. To evaluate whether elevated K-Ras and c-Myc protein levels were due to *let-7*-mediated derepression, we selectively overexpressed *let-7g* and measured the effects on luciferase-based reporter constructs carrying the 3′ UTRs of K-Ras and c-Myc (**Supplementary Fig. 5**). Consistent with previous studies[13], we observed robust repression of the K-Ras 3′ UTR as a result of *let-7* overexpression (**Fig. 3b**). In addition, the c-Myc 3′ UTR was also repressed in this setting, suggesting that both oncogenes are *let-7* targets. Similarly, 2′-*O*-methyl oligonucleotides complementary to *let-7g* caused derepression of the 3′ UTRs of K-Ras and c-Myc (**Supplementary Fig. 5**). Moreover, both oncogenes are direct *let-7* targets, as mutation of the *let-7* binding sites in the K-Ras and c-Myc 3′ UTRs caused derepression comparable to *let-7* inhibition (**Supplementary Fig. 5**). To examine the role of *let-7* family members in transformation, LKR13 cells were transfected with 2′-*O*-methyl oligonucleotides complementary to *let-7g*. We observed an elevation in

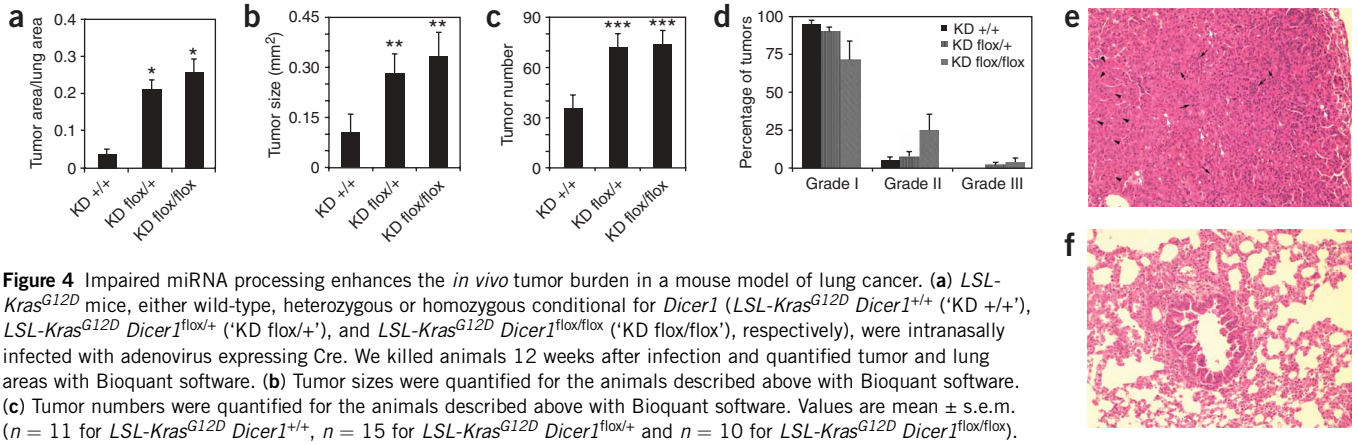


**Figure 4** Impaired miRNA processing enhances the *in vivo* tumor burden in a mouse model of lung cancer. (**a**) *LSL-*$Kras^{G12D}$ mice, either wild-type, heterozygous or homozygous conditional for *Dicer1* (*LSL-*$Kras^{G12D}$ $Dicer1^{+/+}$ ('KD +/+'), *LSL-*$Kras^{G12D}$ $Dicer1^{flox/+}$ ('KD flox/+'), and *LSL-*$Kras^{G12D}$ $Dicer1^{flox/flox}$ ('KD flox/flox'), respectively), were intranasally infected with adenovirus expressing Cre. We killed animals 12 weeks after infection and quantified tumor and lung areas with Bioquant software. (**b**) Tumor sizes were quantified for the animals described above with Bioquant software. (**c**) Tumor numbers were quantified for the animals described above with Bioquant software. Values are mean ± s.e.m. ($n = 11$ for *LSL-*$Kras^{G12D}$ $Dicer1^{+/+}$, $n = 15$ for *LSL-*$Kras^{G12D}$ $Dicer1^{flox/+}$ and $n = 10$ for *LSL-*$Kras^{G12D}$ $Dicer1^{flox/flox}$). *, $P < 5 \times 10^{-5}$, **, $P < 0.05$; ***, $P < 0.005$. (**d**) Tumors from animals of the genotypes described above were scored for histological grade using a grading scheme described previously (see Methods). Values are mean ± s.e.m. ($n = 5$ for each genotype). (**e**) Hematoxylin/eosin staining of a Grade III tumor from a *LSL-*$Kras^{G12D}$ $Dicer1^{flox/+}$ animal. Original magnification, 20×. Black arrows indicate areas of nuclear pleomorphism. Arrowheads indicate areas with prominent nucleoli. White arrows indicate areas of vacuolation. (**f**) Hematoxylin/eosin staining of bronchiolar hyperplasia from a *LSL-*$Kras^{G12D}$ $Dicer1^{flox/flox}$ animal. Original magnification, 20×.

growth rate with *let-7* inhibition (**Fig. 3c**). Moreover, overexpression of *let-7g* in miRKD LKR13 cells led to substantial reduction in low-density colony-forming ability (**Supplementary Fig. 5**). Finally, in miRKD human cancer cells, we noted an enrichment of *let-7* family members among the miRNAs whose repression correlates best with heightened transformation (**Supplementary Table 2** online). However, it is also possible that other miRNAs whose repression correlates with enhanced transformation might function in a similar way.

To understand the significance of these findings *in vivo*, we assessed the role of impaired miRNA processing in a mouse model of lung tumorigenesis, using the conditional, activatable allele of *Kras*, *LSL-Kras*$^{G12D}$ (ref. 10). Intranasal infection of *LSL-Kras*$^{G12D}$ mice with adenovirus expressing Cre has been shown to induce non–small cell lung cancer in these mice, with complete penetrance and a defined time course[14]. By crossing *LSL-Kras*$^{G12D}$ mice with mice bearing a conditional knockout allele of *Dicer1* (ref. 6), we generated *LSL-Kras*$^{G12D}$ mice that were wild-type, heterozygous or homozygous for the conditional allele for *Dicer1* (hereafter referred to as *LSL-Kras*$^{G12D}$ *Dicer1*$^{+/+}$, *LSL-Kras*$^{G12D}$ *Dicer1*$^{flox/+}$ and *LSL-Kras*$^{G12D}$ *Dicer1*$^{flox/flox}$, respectively).

We infected this cohort of mice with a Cre-expressing adenovirus, and 12 weeks later, we observed an increase in tumor burden in the *LSL-Kras*$^{G12D}$ *Dicer1*$^{flox/+}$ and *LSL-Kras*$^{G12D}$ *Dicer1*$^{flox/flox}$ mice compared with the *LSL-Kras*$^{G12D}$ *Dicer1*$^{+/+}$ mice. This tumor burden was reflected in substantial increases in the ratio of tumor area to lung area (**Fig. 4a**), tumor size (**Fig. 4b**) and tumor number (**Fig. 4c**). We also performed histological grading analysis of tumors from *LSL-Kras*$^{G12D}$ *Dicer1*$^{+/+}$, *LSL-Kras*$^{G12D}$ *Dicer1*$^{flox/+}$ and *LSL-Kras*$^{G12D}$ *Dicer1*$^{flox/flox}$ mice. Overall, we noted a slight shift in grade in the *Dicer1* mutant mice, with the highest-grade lesions only present in the *LSL-Kras*$^{G12D}$ *Dicer1*$^{flox/+}$ and *LSL-Kras*$^{G12D}$ *Dicer1*$^{flox/flox}$ mice (**Fig. 4d**). These lesions had areas of nuclear pleomorphism, prominent nucleoli and significant vacuolation (**Fig. 4e**). In addition, the *LSL-Kras*$^{G12D}$ *Dicer1*$^{flox/+}$ and *LSL-Kras*$^{G12D}$ *Dicer1*$^{flox/flox}$ mice showed more extensive bronchiolar hyperplasia than *LSL-Kras*$^{G12D}$ *Dicer1*$^{+/+}$ mice (**Fig. 4f**), further demonstrating the enhanced tumor burden in *Dicer1* mutant mice. In total, these results suggest that impaired miRNA processing can enhance tumorigenesis *in vivo* through an enhanced tumor burden.

These studies demonstrate that impaired miRNA biogenesis accelerates oncogenic transformation through the deregulation of target oncogenes. Previous work has shown that both human and mouse cancers show a global reduction of mature miRNA levels compared with normal tissues[3]. Our work demonstrates that this reduced mature miRNA expression can promote tumorigenesis. Notably, the loss of miRNA processing, though incomplete, causes a marked change in the transformed phenotype of cancer cells. Furthermore, our results are consistent with observations correlating reduced Dicer1 expression in a subset of non–small cell lung cancers with poor prognosis[15]. These findings are also consistent with work showing the *let-7* family as a negative regulator of the Ras family of oncogenes[13], while extending its role in oncogenic transformation to c-Myc. Of note, previous studies have implicated specific miRNAs as oncogenes, as their overexpression accelerates tumorigenesis[16–20]. Our study does not directly contradict these findings but rather suggests that overall repression of miRNAs can enhance tumorigenesis. Recent work has also shown that the global repression of miRNAs in human cancers does not coincide with reductions in the primary miRNA transcripts, suggesting that altered regulation of the miRNA processing machinery occurs in human cancers[21]. Taken as a whole, these investigations highlight a functional role for miRNA biogenesis in tumorigenesis.

## METHODS

**Cell culture.** Human cancer cell lines (HCA7, MCF7, U2OS) were originally obtained from ATCC. LKR13 cells were generated from a mouse lung adenocarcinoma[4,5]. Wild-type and *LSL-Kras*$^{G12D}$ MEFs were generated as described previously[10]. Cells were maintained using standard conditions.

**Transformation, immortalization, growth and tumorigenesis assays.** Transformation, immortalization, growth and tumorigenesis assays were performed essentially as described[22].

**5-bromodeoxyuridine (BrdU) and cell-cycle profile analysis.** Anti-BrdU and 7-amino-actinomycin D (AAD) staining was analyzed by flow cytometry according to the manufacturer's instructions (BD Biosciences).

**Invasion assays.** Invasion assays were performed using a 24-well collagen-based cell invasion assay according to the manufacturer's instructions (Chemicon).

**shRNA design and infection.** shRNAs were designed and cloned, and cells were infected with them, as described previously[9,23]. Subsequent adenovirus infection of shRNA-expressing cells was performed as described[9].

**RNA blotting.** Small RNA blotting was performed as described[9].

**Immunoblotting assays.** Immunoblotting was performed as described[22].

**Quantitative reverse transcription (Q-RT) PCR.** Q-RT PCR of mouse DGCR8, Drosha, Dicer1, K-Ras and c-Myc was performed as before[24]. Q-RT PCR of satellite repeat transcripts was performed as described[25].

**miRNA overexpression and repression assays.** We cloned *let-7g* miRNA and seed mutant *let-7e* miRNA into MSCV-neo (Clontech) with approximately 500 bp of flanking sequence. 2′-*O*-methyl oligonucleotides complementary to *let-7g* and miR-181a were synthesized commercially (Integrated DNA Technologies). Overexpression vectors and 2′-*O*-methyl oligonucleotides were transfected into cells using previously described methods[26,27].

**Luciferase assays.** Mouse K-Ras (EMBL accession number BC004642) and c-Myc (EMBL accession number X01023) 3′ UTRs were cloned into *Renilla* luciferase vectors described previously, and luciferase assays were performed as before[28].

**miRNA expression analysis.** miRNA expression profiling was performed using a bead-based miRNA detection platform as previously described with modifications[3] (**Supplementary Methods** online).

**Mice.** *LSL-Kras*$^{G12D}$ mice[10] were cross-bred to *Dicer1*$^{flox/flox}$ mice[6] to generate *LSL-Kras*$^{G12D}$ *Dicer1*$^{flox/+}$ mice, which were subsequently interbred to produce the experimental cohort. Research was approved by the Committee for Animal Care of the Massachusetts Institute of Technology and was conducted in compliance with the Animal Welfare Act Regulations and other federal statutes relating to animals and experiments involving animals and adheres to the principles set forth in the 1996 National Research Council Guide for Care and Use of Laboratory Animals (institutional animal welfare assurance number, A-3125-01).

**Intranasal infection and tumor analysis.** Mice were infected intranasally with adenovirus expressing Cre as described[14]. Twelve weeks after infection, mice were killed, and lungs were collected, fixed in formalin and stained for histology as described previously[14]. Lung and tumor areas were determined using Bioquant Image Analysis software, as described previously[29].

**Tumor grading analysis.** Tumor grading was done without knowledge of genotype, as described previously[29]. Each tumor was given a score of 1 to 3 based on predetermined criteria (**Supplementary Methods**).

**Requests for materials.** tjacks@mit.edu

*Note: Supplementary information is available on the Nature Genetics website.*

**ACKNOWLEDGMENTS**

We thank R. Shiekhattar for the Flag-Dicer1 cDNA construct; V.N. Kim for the Flag-DGCR8 and Flag-Drosha cDNA constructs and P.A. Sharp for the pRL-TK

and pGL3 constructs. We thank A. Ventura, P. Sandy, M. Winslow, H. Zhang and members of the Sharp laboratory for experimental advice and assistance. We also thank R. Bronson and M.E. McLaughlin for histological analysis. We acknowledge C. Bender Kim, M. Winslow, C. Reinhardt and S. Kissler for critical review of the manuscript. This work was supported by grant 2-PO1-CA42063-21 from the National Cancer Institute and by Cancer Center Support grant P30-CA14051 from the National Cancer Institute. M.S.K. is an NSF Graduate Research Fellow. T.J. is a Ludwig Scholar. T.R.G. and T.J. are investigators of the Howard Hughes Medical Institute.

**AUTHOR CONTRIBUTIONS**

M.S.K. and J.L. conceived the project. M.S.K., J.L. and K.L.M. carried out all experiments described. T.R.G. and T.J. supervised the experimental work and interpretation of data. The manuscript was prepared by M.S.K. and T.J.

**COMPETING INTERESTS STATEMENT**

The authors declare no competing financial interests.

Published online at http://www.nature.com/naturegenetics
Reprints and permissions information is available online at http://npg.nature.com/reprintsandpermissions

1. Bartel, D.P. MicroRNAs: genomics, biogenesis, mechanism, and function. *Cell* **116**, 281–297 (2004).
2. Gregory, R.I. & Shiekhattar, R. MicroRNA biogenesis and cancer. *Cancer Res.* **65**, 3509–3512 (2005).
3. Lu, J. *et al.* MicroRNA expression profiles classify human cancers. *Nature* **435**, 834–838 (2005).
4. Wislez, M. *et al.* High expression of ligands for chemokine receptor CXCR2 in alveolar epithelial neoplasia induced by oncogenic kras. *Cancer Res.* **66**, 4198–4207 (2006).
5. Johnson, L. *et al.* Somatic activation of the K-ras oncogene causes early onset lung cancer in mice. *Nature* **410**, 1111–1116 (2001).
6. Harfe, B.D., McManus, M.T., Mansfield, J.H., Hornstein, E. & Tabin, C.J. The RNaseIII enzyme Dicer is required for morphogenesis but not patterning of the vertebrate limb. *Proc. Natl. Acad. Sci. USA* **102**, 10898–10903 (2005).
7. Kanellopoulou, C. *et al.* Dicer-deficient mouse embryonic stem cells are defective in differentiation and centromeric silencing. *Genes Dev.* **19**, 489–501 (2005).
8. Murchison, E.P., Partridge, J.F., Tam, O.H., Cheloufi, S. & Hannon, G.J. Characterization of Dicer-deficient murine embryonic stem cells. *Proc. Natl. Acad. Sci. USA* **102**, 12135–12140 (2005).
9. Ventura, A. *et al.* Cre-lox-regulated conditional RNA interference from transgenes. *Proc. Natl. Acad. Sci. USA* **101**, 10380–10385 (2004).
10. Tuveson, D.A. *et al.* Endogenous oncogenic K-ras(G12D) stimulates proliferation and widespread neoplastic and developmental defects. *Cancer Cell* **5**, 375–387 (2004).
11. Adhikary, S. & Eilers, M. Transcriptional regulation and transformation by Myc proteins. *Nat. Rev. Mol. Cell Biol.* **6**, 635–645 (2005).
12. John, B. *et al.* Human MicroRNA targets. *PLoS Biol.* **2**, e363 (2004).
13. Johnson, S.M. *et al.* RAS is regulated by the let-7 microRNA family. *Cell* **120**, 635–647 (2005).
14. Jackson, E.L. *et al.* Analysis of lung tumor initiation and progression using conditional expression of oncogenic K-ras. *Genes Dev.* **15**, 3243–3248 (2001).
15. Karube, Y. *et al.* Reduced expression of Dicer associated with poor prognosis in lung cancer patients. *Cancer Sci.* **96**, 111–115 (2005).
16. Hayashita, Y. *et al.* A polycistronic microRNA cluster, miR-17–92, is overexpressed in human lung cancers and enhances cell proliferation. *Cancer Res.* **65**, 9628–9632 (2005).
17. He, L. *et al.* A microRNA polycistron as a potential human oncogene. *Nature* **435**, 828–833 (2005).
18. O'Donnell, K.A., Wentzel, E.A., Zeller, K.I., Dang, C.V. & Mendell, J.T. c-Myc-regulated microRNAs modulate E2F1 expression. *Nature* **435**, 839–843 (2005).
19. Ota, A. *et al.* Identification and characterization of a novel gene, C13orf25, as a target for 13q31-q32 amplification in malignant lymphoma. *Cancer Res.* **64**, 3087–3095 (2004).
20. Volinia, S. *et al.* A microRNA expression signature of human solid tumors defines cancer gene targets. *Proc. Natl. Acad. Sci. USA* **103**, 2257–2261 (2006).
21. Thomson, J.M. *et al.* Extensive post-transcriptional regulation of microRNAs and its implications for cancer. *Genes Dev.* **20**, 2202–2207 (2006).
22. Sage, J. *et al.* Targeted disruption of the three Rb-related genes leads to loss of G(1) control and immortalization. *Genes Dev.* **14**, 3037–3050 (2000).
23. Brummelkamp, T.R., Bernards, R. & Agami, R. A system for stable expression of short interfering RNAs in mammalian cells. *Science* **296**, 550–553 (2002).
24. Sweet-Cordero, A. *et al.* An oncogenic KRAS2 expression signature identified by cross-species gene-expression analysis. *Nat. Genet.* **37**, 48–55 (2005).
25. Martens, J.H. *et al.* The profile of repeat-associated histone lysine methylation states in the mouse epigenome. *EMBO J.* **24**, 800–812 (2005).
26. Hutvagner, G., Simard, M.J., Mello, C.C. & Zamore, P.D. Sequence-specific inhibition of small RNA function. *PLoS Biol.* **2**, E98 (2004).
27. Meister, G., Landthaler, M., Dorsett, Y. & Tuschl, T. Sequence-specific inhibition of microRNA- and siRNA-induced RNA silencing. *RNA* **10**, 544–550 (2004).
28. Doench, J.G., Petersen, C.P. & Sharp, P.A. siRNAs can function as miRNAs. *Genes Dev.* **17**, 438–442 (2003).
29. Jackson, E.L. *et al.* The differential effects of mutant p53 alleles on advanced murine lung cancer. *Cancer Res.* **65**, 10280–10288 (2005).